

High- T_c Superconducting Step-Edge Junction on Sapphire Fabricated by Non-Etching Technique

Alexander D. Mashtakov, Gennady A. Ovsyannikov, Igor V. Borisenko, Karen Y. Constantinyan, Iosif M. Kotelyanskii
Institute of Radio Engineering and Electronics RAS, Moscow 103907, Russia

Donats Erts
Chalmers University of Technology, Gothenburg S-41296, Sweden

Abstract—We have produced step-edge Josephson junctions on steps in an epitaxially grown CeO_2 layer on r-cut sapphire. The epitaxial CeO_2 layer is deposited at high temperature through a MgO/CeO_2 micromask. The optimum orientation of the step flank (FS) for grain boundary junction was determined on the basis of known experimental data of $\text{YBa}_2\text{Cu}_3\text{O}_x$ (YBCO) film growth on tilted substrates and from analyses of bicrystal grain boundaries formed in YBCO films along the boundary between the FS and planar substrate. Atomic force microscopy (AFM) observations of the steps in which the FS was parallel to the $[110]\text{CeO}_2$ plane show that the slope angles is in a range from 50° to 70° that correspond to (111) and $(221)\text{CeO}_2$ crystallographic planes. The results of dc and microwave measurements of obtained high- T_c step-edge junction are presented.

I. INTRODUCTION

For step-edge junction fabrication a high- T_c film is deposited on a substrate in which a deep step is present [1], [2]. Along the step flank (FS) the high- T_c film grows in an orientation different from that grown on the planar part of substrate. The conventional method of step formation in a substrate is an ion milling. Recently we proposed a new approach for step-edge formation using a micromask technique in conjunction with the deposition of an epitaxial CeO_2 layer [2], [3]. The technique allows for a controlled growth of the FS with predetermined orientation. In this paper we present experimental data on step-edge junctions on CeO_2 -buffered sapphire substrates made by non-etching technique. Results for several crystallographic orientations of FS are discussed

II. TYPES OF GRAIN BOUNDARIES IN STEP-EDGE JUNCTION ON SAPPHIRE

The following crystallographic orientation are obtained with c-oriented YBCO grown on CeO_2 -buffered r-cut sapphire $(001)\text{YBCO}/(001)\text{CeO}_2/(1\bar{1}02)\text{Al}_2\text{O}_3$, $[100]\text{YBCO}/[110]\text{CeO}_2/[2021]\text{Al}_2\text{O}_3$, [4]. We try to predict the type of grain boundary (GB) between YBCO epitaxial

Manuscript received September 15, 1998.

This work was supported in part by the Russian State Program "Modern Problems of the Solid State Physics", "Superconductivity" division, Russian Foundation for Basic Research, INTAS and INCO-Copernicus programs of the EU, NATO research program and Russian-Sweden Academic project.

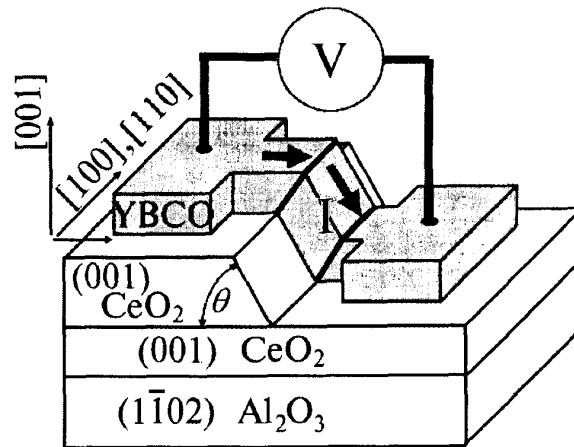


Fig. 1. Geometry of step-edge junction on sapphire for $\text{FS}/[010]\text{CeO}_2$.

film on a flat surface and on the FS by using already known experimental data for YBCO film growth on tilted substrates [5]-[7] and to determinate the preferable orientation of the FS that results in the best junction quality. We will analyze two cases: (1) the FS is parallel to the $[010]\text{CeO}_2$ and (2) $[110]\text{CeO}_2$. The FS is tilted at an angle θ (see Fig. 1).

A. Flank of Step is Parallel to $[010]\text{CeO}_2/[1120]\text{Al}_2\text{O}_3$

By changing the angle θ the FS passes through several CeO_2 crystallographic planes. We will analyze the cases corresponding to a FS with small crystallographic indices. At low angles, $0^\circ < \theta < 30^\circ$, the epitaxial YBCO film grows on FS with the same orientation as on $(001)\text{CeO}_2$ [7]. So for $\theta < 30^\circ$ the misorientation angle α between the c-axes of the films on the flat plane and on the FS is zero ($\alpha=0$). In the opposite case ($\theta=90^\circ$) the FS is parallel to the $(100)\text{CeO}_2$ plane, on which the YBCO film grows with the same orientation as on $(001)\text{CeO}_2$. Thus a 90° basal-plane-faced tilt (BFT) GB ($\alpha=90^\circ$) is formed [1], [5]. Experiments [5] show that 90° BFT GBs without defects limit superconducting critical current density j_c (approximately one order of magnitude smaller than that of $(001)\text{YBCO}$) similar to a-oriented film but with a very weak j_c magnetic field dependence.

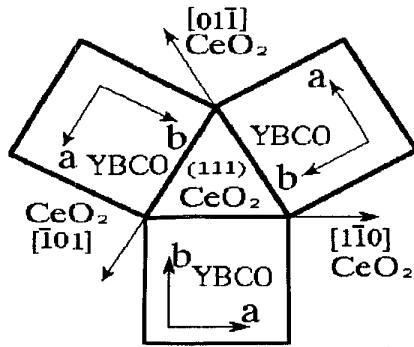


Fig. 2. Schematic diagram of a growth of (001)YBCO on (111)CeO₂: #1 [010]YBCO//[110]CeO₂, #2 [010]YBCO//[101]CeO₂, #3 [010]YBCO//[011]CeO₂.

For $\theta=45^\circ$ the FS is parallel to the (101)CeO₂ plane. In analogy with YBCO growth on a (110)SrTiO₃ substrate [5], the YBCO film grows on (101) CeO₂ possibly with two orientations: (110) and (103), depending on growth conditions. Formed GBs could be realized by the transformation $45^\circ[110]$ BFT for (110)YBCO ($\alpha=45^\circ$) and $45^\circ[110]$ BFT subsequent by $90^\circ[110]$ twist (TW) transformation for (103)YBCO orientation on FS. The last transformation is obtained by rotation of the c-oriented grain about an axis, normal to the GB border plane. According to measurements [5] TW GB does not limit critical current density. In analogy with in-plane tilted (IT) GBs we propose that GBs $\theta=45^\circ$ boundary will produce low current density junctions.

B. Step Flank is Parallel to $[110]$ CeO₂// $[1011]$ Al₂O₃

The results of this case is presented in table I. The $\theta=90^\circ$ is very close to that of the case FS//[010]CeO₂, $\theta=45^\circ$. Experimental investigation of YBCO growth on (111) CeO₂ ($\theta=54.7^\circ$) shows three domains of (001)YBCO film with 60° tilting in the a-b plane as shown in Fig.2 [6]. Misorientation of the c-axis is $\alpha=54.7^\circ$ with the YBCO a and b axes tilted around the [001] direction. At $\theta=70.5^\circ$ the FS coincides with the (221)CeO₂ plane which can be decomposed as a translation of $\langle 110 \rangle$ CeO₂ with period $a\sqrt{2}$ (close to YBCO

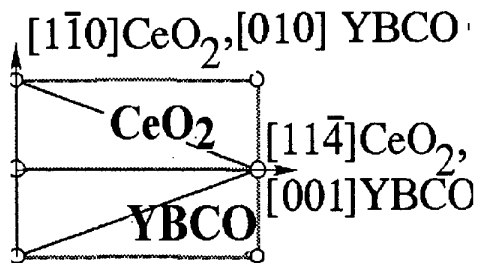


Fig.3. Schematic diagram of a growth of (001)YBCO on (221)CeO₂: [010]YBCO//[110]CeO₂, [001]YBCO//[114]CeO₂.

a-axis parameter) and translation along $\langle 114 \rangle$ CeO₂ with a period $1.5a\sqrt{2}$ (which differs from YBCO c-axis lattice constant by 0.8%), where $a=0.541$ nm is the CeO₂ lattice parameter. We propose that (100)YBCO grows on (221)CeO₂ with epitaxial sequence [010]YBCO//[110]CeO₂, [001]YBCO//[114]CeO₂ (see Fig. 3). GB with $\alpha=19.4^\circ$ could be obtained with the following transformation $19.4^\circ[110]$ BFT. We try to realize the case FS// $\{110\}$ CeO₂ in our experiment.

TABLE I
TYPES OF GB FOR STEP-EDGE JUNCTION ON SAPPHIRE WITH
FS//[110]CeO₂// $[1011]$ Al₂O₃

θ ,FS	YBCO orientations	Types of GB
54.7° (111)		#1 54.7°[010] BFT #2 54.7°[010]BFT + 60° [001]IT #3 54.7°[010] BFT+ 120°[001]IT
70.5° (221)		19.4°[110]BFT
90° (110)		45°[001]IT + 90°[100]TW
		45°[010] BFT

III. EXPERIMENTAL TECHNIQUE

The whole surface of the r-plane sapphire (Al₂O₃) with (1102) orientation is covered with an epitaxial CeO₂ buffer layer to prevent the diffusion of Al atoms from the sapphire into YBCO film during its deposition at high temperature (see Fig.4). An epitaxial (001)CeO₂ film with thickness 30-60 nm is deposited on the sapphire substrate with RF-magnetron sputtering from Ce metal target [4]. The process of CeO₂ step preparation starts with patterning of a 1 μ m thick photoresist mask using photolithography techniques. The edge of the photoresist mask, which fixes the position of the step edge is aligned with $[110]$ CeO₂// $[2021]$ Al₂O₃. An amorphous CeO₂/MgO bilayer film is deposited with RF

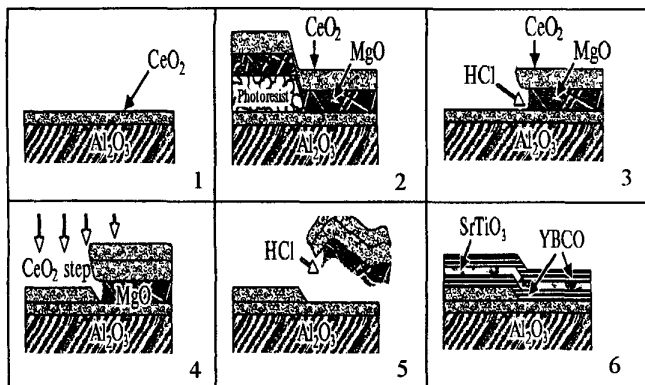


Fig.4. Technology procedures: 1. Deposition of 50 nm CeO_2 buffer layer on r-plane Al_2O_3 . 2. Photolithography; amorphous $\text{MgO}+\text{CeO}_2$ micromask deposition. 3. Lift-off process of photoresist; undercutting of micromask at 0.5% vol. HCl solution. 4. Step formation by magnetron deposition at high temperature. 5. Removing the CeO_2/MgO micromask at HCl solution. 6. YBCO film with extra: $\text{SrTiO}_3/\text{YBa}_2\text{Cu}_3\text{O}_x$ buffer layer deposition.

magnetron sputtering at room temperature. The bilayer mask edge is formed by ultrasonic stimulated lift-off in acetone. To increase the undercut in the mask, the CeO_2/MgO film was developed in solution of 0.5% vol. HCl solution. After growth of the 30-300 nm thick "step" (001) CeO_2 layer at high temperature the bilayer mask was removed in acid.

The 100-200 nm thick superconducting (001)YBCO film was deposited by laser ablation and by DC-sputtering at high oxygen pressure [2],[3]. The 700°-800°C deposition temperature was held constant while the oxygen pressure was 4 mbar for DC-sputtering and 0.6-1.0 mbar for laser

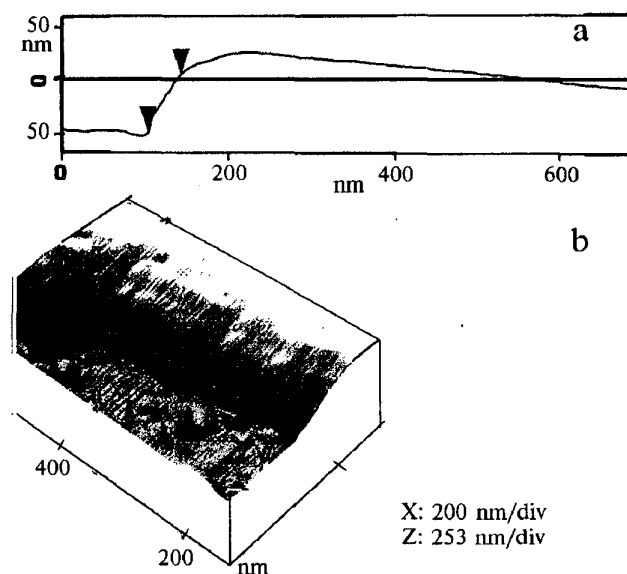


Fig.5. AFM cross-section and 3-dimensional image of CeO_2 step. Slope angle between marks on cross-section is equal to 54°.

ablation. A $\text{SrTiO}_3/\text{YBCO}$ buffer bilayer was used in some cases for reducing YBCO interaction with CeO_2 on the FS [3], [4]. Four μm wide Josephson junctions in the form of narrow bridges in the YBCO film across the step were fabricated by both by wet and ion beam etching through a photoresist mask. All electrical measurements were made with the four-probe method.

IV. EXPERIMENTAL RESULTS

Step profiles were investigated by atomic force microscope (AFM) using a Si tip. Using scanning electron microscope, our estimation of the tip shape indicates that it is possible to measure the surface irregularities with a tilt angle less than 70°. AFM investigation shows that the step edge irregularities are about 200 nm which is of the same order that photolithography can provide. A 50° to 70° variation in tilt angle θ was observed along the step slope (Fig.5). According to our estimations the FS should consist of (111) and (221) CeO_2 crystallographic planes.

The YBCO films on the flat surfaces of the sample have a zero resistance temperature $T_{c0} = 89 \pm 90$ K with a transition width of less than 1 K. The 77K critical current density at exceeds $5 \cdot 10^6$ A/cm². The same measurements for the step-crossing bridges (junctions) showed a lower of the superconducting transition temperature $T_{c0}' = 80-84$ K possibly due to the strong influence of thermal fluctuation currents I_f on junction with small critical currents ($I_c \leq I_f$). At $T=65$ K junction critical current densities are 10^4-10^5 A/cm² and the characteristic voltages are $V_0 = I_c R_N = 0.5 - 2$ mV where I_c is critical current and R_N is the (asymptotic) normal resistance.

Two types of I-V curves were observed for the same fabrication techniques. The junctions of the first type have I-V curves with relatively small excess current measured at voltages larger than 1 mV. Josephson coupling in these junctions (Fig.6) is confirm by appearance of Shapiro steps on the I-V curves at voltages corresponding to the harmonics of the microwave frequency ($f_e = 30 - 100$ GHz). At $T=60$ K the maximal height of the first Shapiro step was three times smaller than the value calculated from the RSJ model [8] for the experimental parameter V_0 . Weak dependence of the critical current on magnetic field and subharmonic Shapiro steps indicate on the non-uniform current distribution along the GB.

Junction response as an video detector was investigated at millimeter and submillimeter frequencies. A selective Josephson detection response with the phase flip-over at a voltage bias $V = V_f = \hbar f_e / 2e \approx 0.1$ mV for an applied frequency $f_e = 51.36$ GHz was observed (Fig. 6). The specific shape of the response is caused by partial phase-locking of the Josephson radiation by external monochromatic radiation. The extra peak in the detector response corresponds to subharmonic detection. The 60 K line width of Josephson self radiation $\Delta f = 500$ GHz, determined from

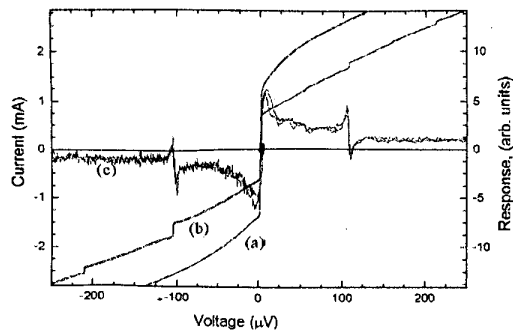


Fig.6. Autonomous (a) and mm wave affected (b) I-V curves of the step-edge junction with pronounced Josephson effect. Detector response of step-edge junction vs voltage(c). Temperature is equal 65K.

the response [8], is 2-3 times greater than that estimated with the RSJ model. About 10% of step-edge junctions fabricated on buffered sapphire have such dc and microwave characteristics.

Junctions of the second type of the had similar I-V curve but higher the excess current (about equal to the critical current) at $V \approx 4$ mV. The dynamic resistance obtained from these I-V curves gradually rises with increasing bias voltage up to value of several millivolts (Fig. 7). I_c values are several time higher than those of the first type of step-edge junctions. No Shapiro steps were observed in this case for external radiation frequency 100 GHz. The I-V curve shape

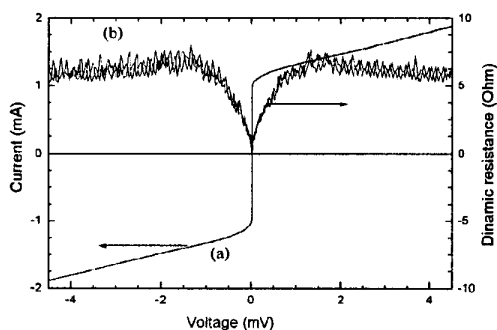


Fig.7. I-V curve(a) and voltage dependence of dynamic resistance (b) for second types of step-edge junction. No Shapiro steps were observed. The critical current was depressed monotonously when microwave power on. Temperature is equal 65K.

corresponds to that obtained [9] from "wavy" step-edge junctions made using a wavy mask to etch the step. The junctions in this case have a higher probability of being shorted by superconducting filaments.

IV. EXPERIMENTAL RESULTS

We have developed a non-etching process for the fabrication of high- T_c the step-edge Josephson junctions. All junctions exhibit non-flux flow I-V curve and Shapiro steps have been observed for 10% of the fabricated junctions. Step shape irregularities resulting in shorting of the grain boundary by superconducting filaments with the size larger the coherence length are the main cause of low reproducibility of these junctions.

ACKNOWLEDGMENT

We thanks Z.G. Ivanov, P.B. Mozhaev and P.V. Komissinskii for help in experiment and fruitful discussion. The Swedish nanolab is acknowledge for the processing of laser ablated YBCO film.

REFERENCES

- [1] K. Herrmann, G. Kunkel, M. Siegel, J. Schubert, W. Zander, A.I. Braginski et al, "Correlation of YBCO step-edge junction characteristics with microstructure," *J. Appl. Phys.*, vol.78, pp.1131-1139, 1995.
- [2] I.M. Kotelyanski, A.D. Mashtakov, P.B. Mozhaev, G.A. Ovsyannikov, Yu.M. Dikaev, D. Ertz, "Non-etching high- T_c step-edge Josephson junction on sapphire substrate," *Inst. Phys. Conf. Ser.No148, 1995 Europ. Conf. on Appl. Superc.*, vol.2, pp.1375-1378, 1995.
- [3] G.A. Ovsyannikov, A.D. Mashtakov, I.M. Kotelyanski, P.B. Mozhaev, K.Y. Constantinian, Z.G. Ivanov, D. Ertz. "New Technique in Fabrication of High- T_c Superconducting Step-Edge Junction." *Extend. Abstracts of ISEC '97, Germany*, vol.2, p.76-78, 1997.
- [4] A D Mashtakov, I M Kotelyanskii, V A Luzanov, P B Mozhaev, G A Ovsyannikov, "Temperature restriction for $YBa_2Cu_3O_x$ thin film deposition on CeO_2 buffer layer" *Inst. Phys. Conf. Ser. No158*, pp.229-231, 1997.
- [5] Eom C B, A.F. Marshall, Y.Suzuki, T.H. Geballe, B. Boyer, R.F.W. Pease et al, "Growth mechanisms and properties of 90° grain boundary in YBCO thin films", *Phys. Rev.B*, vol.46, pp.11902-11913, 1992.
- [6] I.M. Kotelyanski, V.A. Lusanov, Yu.M. Dikaev, V.B. Kravchenko, B.T. Melikh, "Deposition of epitaxial CeO_2 film with different border on sapphire substrate", *Thin Solid Films*, vol. 280, pp. 163-166, 1996.
- [7] Y.Y. Divin, U Popper, P.M. Shadrin, et al, "YBCO thin films with tilted c-axis as base electrodes of high- T_c planar junctions," *Inst. Phys. Conf. Ser.No148, 1995 Europ. Conf. on Appl. Superc.*, vol.2, pp.1359-1362, 1995.
- [8] K.Y. Constantinian, G. A. Ovsyannikov, A. D. Mashtakov, J. Ramos, Z.G. Ivanov, J. Mygind, N.F. Pedersen. "Microwave dynamics of YBCO bi-epitaxial Josephson structures," *Physica C*, vol.273, pp.21029, 1996.
- [9] H.R. Yi, D. Winkler, Z.G. Ivanov, T. Claeson, "Electron beam lithographed straight and wavy YBCO step-edge junctions", *IEEE Tr. Appl. Superconductivity*, vol.5, pp.2778-2781, 1995.